European Journal of Chemistry

Journal webpage: www.eurjchem.com

Synthesis, characterization, mass spectral fragmentation, thermal study and biological evaluation of new Schiff base ligand and its metal(II) complexes derived from 4-(diethylamino)salicylaldehyde and thiazole moiety

Nagesh Gunvanthrao Yernale [1], Mahadev Dhanraj Udayagiri [2] and Bennikallu Hire Mathada Mruthyunjayaswamy [1,*]

[1] *Department of Studies and Research in Chemistry, Gulbarga University, Kalaburagi, 585106, Karnataka, India*
[2] *Government Degree College, Sedam Road, Kalaburagi, 585106, Karnataka, India*

** Corresponding author at: Department of Studies and Research in Chemistry, Gulbarga University, Kalaburagi, 585106, Karnataka, India. Tel.: +91.944.8830318. Fax: +91.08472.245632. E-mail address: bhmmswamy53@rediffmail.com (B.H.M. Mruthyunjayaswamy).*

ARTICLE INFORMATION

DOI: 10.5155/eurjchem.7.1.56-65.1372

Received: 24 November 2015
Received in revised form: 18 December 2015
Accepted: 19 December 2015
Published online: 31 March 2016
Printed: 31 March 2016

KEYWORDS

Thiazole
Schiff base
Mass fragmentation
Antibacterial activity
Transition metal complexes
4-(Diethylamino)salicylaldehyde

ABSTRACT

A new Schiff base ligand, 2-(4-(diethylamino)-2-hydroxybenzylidene)-*N*-(4-phenylthiazol-2-yl) hydrazinecarboxamide (L) and its copper(II), cobalt(II), nickel(II) and zinc(II) complexes were prepared and characterized by analytical and spectroscopic methods. The analytical data suggests the composition of the metal complexes to be 1:2 of the type [ML_2] for copper(II), cobalt(II) and nickel(II) complexes and 1:1 stoichiometry of the type [MLCl] for zinc(II) complex, where L is the deprotonated Schiff base ligand. The conductance measurement data indicates that all the metal complexes are non-electrolytes. The antioxidant activity of all the compounds was evaluated using the DPPH assay. The Schiff base ligand (L) and its copper(II), cobalt(II) complexes are found to be good antioxidants. The antibacterial and antifungal activity was performed by agar diffusion methods. All the metal(II) complexes inhibited the growth of bacteria and fungi. Also, brine shrimp bioassay was also carried out to study the *in vitro* cytotoxic properties, the copper(II) and zinc(II) complexes showed good cytotoxic property.

Cite this: *Eur. J. Chem.* **2016**, *7(1)*, 56-65

1. Introduction

Schiff bases have played an important role as chelating ligands in main group and transition metal coordination chemistry because of their stability under a various conditions and also imine ligands are borderline Lewis bases [1]. The important physical and biological properties of Schiff bases are directly correlated to intermolecular hydrogen bonding and proton transfer equilibria [2]. Schiff bases also offer opportunities for inducing substrate chirality, tuning metal-centered electronic factors and enhancing the solubility and stability of homogeneous or heterogeneous catalysts [3]. Transition metals are involved in a number of biological processes which are essential for life. The metal ions can coordinate with hetero atom (O or N) terminals from proteins in a variety of models and play a crucial role in the conformation and function of biological macromolecules [4,5]. In the field of bioinorganic chemistry, interest in Schiff bases and their metal complexes has centered on the role of such complexes in providing synthetic models for the metal-containing sites in metallo-proteins and metallo-enzymes [6].

Furthermore, the tridentate Schiff base ligands and their metal complexes are increasingly important for designing metal complexes related to synthetic and natural oxygen carriers. Copper complexes of tridentate Schiff base with dimeric units are considered as bioinorganic model compounds [7]. In recent years, there have been intense investigations of different classes of thiazole derivatives [8,9]. Many of these possess interesting biological properties such as antimicrobial and analgesic activities. Thiazole and its derivatives as ligands with potential sulfur atom are interesting and have gained special attention not only because of their structural chemistry, but also for their importance in medicinal and pharmaceutical field [10,11]. Schiff bases represent an important class of compounds because they are utilized as starting materials in the synthesis of industrial products [12].

In this article, we report here the synthesis and characterization of new Schiff base ligand, 2-(4-(diethyl amino)-2-hydroxybenzylidene)-*N*-(4-phenylthiazol-2-yl) hydrazinecarboxamide (L) containing carbonyl, azomethine

ISSN 2153-2249 (Print) / ISSN 2153-2257 (Online)
http://dx.doi.org/10.5155/eurjchem.7.1.56-65.1372

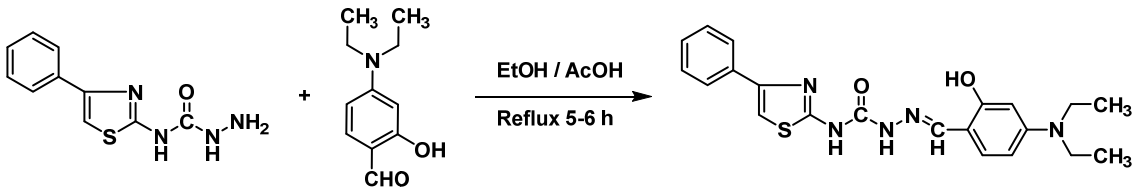

Scheme 1

and hydroxyl groups as chelating sites and its copper (II), cobalt (II), nickel (II) and zinc (II) complexes.

2. Experimental

2.1. Materials and methods

All solvents and chemicals were of commercial reagent grade and used as they are received. The 4-(diethylamino) salicylaldehyde purchased from Sigma Aldrich Chemical company and *N*-(4-phenylthiazol-2-yl) hydrazinecarboxamide is prepared as per literature methods [13,14].

2.2. Synthesis of 2-(4-(diethylamino)-2-hydroxybenzylide ne)-N-(4-phenylthiazol-2-yl)hydrazinecarboxamide (L)

An equimolar mixture of 4-(diethylamino)salicylaldehyde and *N*-(4-phenylthiazol-2-yl)hydrazinecarboxamide in ethanol (30 mL) was refluxed on water bath for about 5-6 h with an addition of a catalytic amount of glacial acetic acid (2-3 drops). The precipitate which separated during reflux was filtered, washed with hot ethanol and recrystallized from hot 1,4-dioxane to get Schiff base ligand, 2-(4-(diethylamino)-2-hydroxybenzylidene)-*N*-(4-phenylthiazol-2-yl)hydrazinecarboxamide (L) (Yield: 78%). The pathway for the synthesis of Schiff base ligand (L) is presented in Scheme 1.

2-(4-(Diethylamino)-2-hydroxybenzylidene)-N-(4-phenyl thiazol-2-yl)hydrazinecarboxamide (**L**): Color: Yellow. Yield: 78%. M.p.: 284-286 °C. FT-IR (KBr, ν, cm^{-1}): 3400 (OH) (br, phenolic), 3329 (NH) (amide), 3200 (NH) (thiazole), 1699 (C=O) (carbonyl), 1624 (C=N) (azomethine), 1297 (C-O) (phenolic). ^{1}H NMR (400 MHz, DMSO-d_6, δ, ppm): 1.3 (t, 6H, CH_3), 3.2 (q, 4H, CH_2), 6.1-7.8 (m, 9H, ArH), 8.1 (s, 1H, HC=N), 10.6 (s, 1H, thiazole NH), 10.9 (s, 1H, CONH), 11.5 (s, 1H, Phenolic OH). MS (EI, *m/z* (%): 410 (M^{+1}, 48). Anal. calcd. for $C_{21}H_{23}N_5O_2S$: C, 61.59; H, 5.66; N, 17.10. Found: C, 61.64; H, 5.66; N, 17.05%.

2.3. Preparation of metal complexes

Schiff base ligand (L) (0.001 mol) in 20 mL of ethanol and a solution of respective metal chlorides (0.002 mol) in 20 mL of ethanol was refluxed on water bath for about 6-7 h and pH of the reaction mixture adjusted to ca. 7.0-7.5 using sodium acetate (0.5 g) and refluxing continued for about an hour more. The reaction mixture was cooled to room temperature and poured into distilled water. The separated precipitates were filtered off, washed with distilled water, then with hot ethanol to remove any traces of unreacted starting materials and finally dried in a vacuum over fused calcium chloride.

Copper(II) complex: Color: Green. Yield: 59%. M.p.: >300 °C. FT-IR (KBr, ν, cm^{-1}): 3319 (NH) (amide), 3253 (NH) (thiazole), 1663 (C=O) (carbonyl), 1595 (C=N) (azomethine), 1353 (C-O) (phenolic), 553 (M-O), 432 (M-N). MS (EI, *m/z* (%): 880 (M^{+1}, 3). Anal. calcd. for $Cu(C_{21}H_{22}N_5O_2S)_2$: C, 57.29; H, 5.04; N, 15.91; Cu, 7.22. Found: C, 57.34; H, 5.06; N, 15.86; Cu, 7.15%. UV/Vis (DMF, cm^{-1}): 15696, 18146. Λ_m ($S.m^2.mol^{-1}$): 29. μ_{eff} (BM): 1.85.

Cobalt(II) complex: Color: Brown. Yield: 56%. M.p.: >300 °C. FT-IR (KBr, ν, cm^{-1}): 3321 (NH) (amide), 3196 (NH) (thiazole), 1681 (C=O) (carbonyl), 1597 (C=N) (azomethine), 1346 (C-O) (phenolic), 588 (M-O), 450 (M-N). MS (EI, *m/z* (%): 874 (M^{+1}, 16). Anal. calcd. for $Co(C_{21}H_{22}N_5O_2S)_2$: C, 57.59; H, 5.06; N, 15.99; Co, 6.73. Found: C, 57.64; H, 5.06; N, 15.96; Co, 6.79%. UV/Vis (DMF, cm^{-1}): 16692, 20493. Λ_m ($S.m^2.mol^{-1}$): 18. μ_{eff} (BM): 5.06.

Nickel(II) complex: Color: Brown. Yield: 52%. M.p.: >300 °C. FT-IR (KBr, ν, cm^{-1}): 3322 (NH) (amide), 3213 (NH) (thiazole), 1687 (C=O) (carbonyl), 1546 (C=N) (azomethine), 1302 (C-O) (phenolic), 541 (M-O), 455 (M-N). MS (EI, *m/z* (%): 874 (M^+, 7). Anal. calcd. for $Ni(C_{21}H_{22}N_5O_2S)_2$: C, 57.61; H, 5.06; N, 16.00; Ni, 6.70. Found: C, 57.66; H, 5.06; N, 16.06; Co, 6.67%. UV/Vis (DMF, cm^{-1}): 14897, 25117. Λ_m ($S.m^2.mol^{-1}$): 17. μ_{eff} (BM): 2.93.

Zinc(II) complex: Color: Orange. Yield: 74%. M.p.: >300 °C. FT-IR (KBr, ν, cm^{-1}): 3341 (NH) (amide), 3198 (NH) (thiazole), 1617 (C=O) (carbonyl), 1604 (C=N) (azomethine), 1301 (C-O) (phenolic), 533 (M-O), 441 (M-N), 353 (M-Cl). ^{1}H NMR (400 MHz, DMSO-d_6, δ, ppm): 1.3 (t, 6H, CH_3), 3.3 (q, 4H, CH_2), 6.1-8.2 (m, 9H, ArH), 8.4 (s, 1H, HC=N), 11.1 (s, 1H, thiazole NH), 11.9 (s, 1H, CONH). MS (EI, *m/z* (%): 508, 510 (M^+, 3). Anal. calcd. for $ZnC_{21}H_{22}N_5O_2SCl$: C, 49.52; H, 4.35; N, 13.75; Zn, 12.84. Found: C, 49.49; H, 4.36; N, 13.74; Zn, 12.81%. Λ_m ($S.m^2.mol^{-1}$): 30.

2.4. Analysis and physical measurement

The metal and chloride contents of the complexes were estimated gravimetrically as per standard method [15]. Carbon, hydrogen and nitrogen analysis was performed on Vario EL III CHNS analyzer. The IR spectra were recorded on Perkin Elmer Spectrum RX-I FT-IR spectrophotometer. ^{1}H NMR spectra were recorded on Bruker 400 MHz spectrometer using DMSO-d_6 as solvent. ESI mass spectra were recorded on mass spectrometer equipped with an ESI source having a mass range of 4000 amu in quadruple and 20,000 amu in TOF. Electronic spectra were recorded on ELICO SL-164 double beam UV-Visible spectrophotometer (ca. 1×10^{-3} M in DMF). Molar conductivity of metal complexes was measured on Elico-CM, 180 Conductivity Bridge (ca. 1×10^{-3} M DMF). ESR measurement of solid copper (II) complex is carried out on BRUKER Bio Spin spectrometer working at a microwave frequency of 8.75-9.65 GHz using DPPH as reference with field set at 3000 Gauss using tetracynoethylene as the 'g' marker (g = 2.00277). Thermogravimetric analyses data were measured on the Perkin Elmer thermal analyzer in a nitrogen atmosphere with a heating rate of 20 °C/min.

2.5. Biological evaluation

2.5.1. Antibacterial and antifungal activity

The antibacterial and antifungal activity of the newly synthesized Schiff base ligand (L) and its copper(II), cobalt(II), nickel(II) and zinc(II) complexes was performed against *S. aureus* (MTCC 3160) and *E. coli* (MTCC 46) bacteria and *A. flavus* (MTCC 1883) and *A. niger* (MTCC 1881) fungi by agar diffusion methods [16,17]. The above microorganisms were

obtained from the Department of Microbiology and Biotechnology, Gulbarga University, Kalaburagi, Karnataka, India which are previously procured from Institute of Microbial Technology Chandigarh (IMTC), India.

For antibacterial activity, the media were prepared by dissolving Peptone 10 g, NaCl 10 g, Yeast extract 5 g and Agar 20 g in 1000 mL of distilled water. Initially, the stock cultures of bacteria were revived by inoculating in broth media and grown at 37 °C for 18 h. The agar plates were prepared and wells were made in the plate. Further, each plate was inoculated with 18 h old cultures (100 µL, 1×10^{-4} CFU) and spread evenly on the plate. After 20 min, the wells were filled with a test compound and standard antibiotic, ciproflaxacin at different concentrations (25, 50, 100, 250, 500 and 1000 µg/mL). All the plates were incubated at 37 °C for 24 h and the diameter of inhibition zone were measured.

For antifungal activity, the media were prepared by using Czapek-Dox Agar (Composition (g/L) sucrose 30.0; sodium nitrate 2.0; K_2HPO_4 1.0, $MgSO_4.7H_2O$ 0.5; KCl 0.5; $FeSO_4$ 0.01; Agar 20). Initially, the stock cultures were revived by inoculating in broth media and grown at 27 °C for 48 h. The agar plates of the above media were prepared and wells were made in the plate. Each plate was inoculated with 48 h old cultures (100 µL, 1×10^4 CFU) and spread evenly on the plate. After 20 min, the wells were filled with different concentrations (25, 50, 100, 250, 500 and 1000 µg/mL) of test samples and antibiotic, fluconazole. All the plates were incubated at 27 °C for 96 h and the diameter of inhibition zone were noted.

2.5.2. In vitro cytotoxicity study

For the study, Brine shrimp nauplii (*Artemia salina*) were used for cytotoxicity assay and followed the protocol given by *Meyer et al.* [10,18] with some modifications. This method is an efficient and inexpensive and has good correlation with cytotoxic activity. Brine shrimp nauplii eggs were hatched in a shallow rectangular dish (22 × 32 cm) filled with artificial sea water. An unequal partition was made in the dish with the help of punctured device. About 50 mg of eggs was sprinkled into the large compartment, which was darkened and the minor compartment was open to ordinary light. After two days nauplii were collected in a pipette from the lighted side.

The stock solutions of the each test compound (1 mg/mL) were prepared by dissolving 10 mg of each test compound in 10 mL of DMSO, different concentrations of the test compounds were placed in separate vials and final volume is adjusted to 10 mL using artificial sea water. After two days, when shrimp larvae were ready, 10 nauplii were then placed in each vial, after 24 h incubation the vials were observed using a magnifying glass and the number of survivors in each vial was counted. Tests were performed in duplicate and the data were analyzed by a Finney computer program to determine the LD_{50} values [19]. The results were compared with a positive control Bleomycin, an anti-cancer drug.

2.5.4. Antioxidant assay (free radical scavenging activity)

The 2,2-diphenyl-1-picrylhydrazyl (DPPH) free radical scavenging activity evaluations is a standard assay in antioxidant activity studies. It is an efficient and rapid technique for screening the radical scavenging activity of specific compounds [20]. Various concentrations (12.5, 25, 50 and 100 µg/mL) of each test compound and standards butylated hydroxyanisole (BHA) and ascorbic acid (Vitamin C) were taken in different test tubes and adjust the volume to 100 µL by adding distilled DMF. To all the tubes add 5 mL methanolic solution of DPPH (0.1 mM), shaken vigorously and allowed to stand for 30 min at room temperature for incubation. After the completion of incubation period, the scavenging ability determines the antiradical power of an antioxidant by measuring the decrease in the absorbance of DPPH at 517 nm. In the radical form, DPPH shows a maximum absorbance at 517 nm, but on reduction by an antioxidant, the absorption decreases and pale-yellow non radical form is produced through donation of a hydrogen atom to form a stable DPPH molecule. The lower absorbance of the reaction mixture indicates higher free radical scavenging activity. The test was performed with three replicates to obtain mean±S.D. The percentage (%) of inhibition of free radical production from DPPH was calculated using the following mathematical equation:

$$\% \text{ Scavenging of DPPH} = [(\text{Control OD-Sample OD})/\text{Control OD}]\times100 \quad (1)$$

3. Results and discussions

3.1. Chemistry

The synthesized copper(II), cobalt(II), nickel(II) and zinc(II) complexes of L are colored solids, stable at room temperature and possess high melting point (>300 °C). The complexes are insoluble in water and common organic solvents; however, these complexes are soluble to a large extent in DMF and DMSO. Elemental analysis data agree well with the suggested composition of Schiff base ligand (L) and its metal(II) complexes. These data suggest that the metal to ligand stoichiometric ratio of the complexes is 1:2 of the type $[ML_2]$ for copper(II), cobalt(II) and nickel(II) complexes and 1:1 stoichiometry of the type [MLCl] for zinc(II) complex. The results of conductivity measurements are too low to account for any dissociation of the complexes in DMF (17-30 $ohm^{-1}\cdot cm^2\cdot mole^{-1}$). Hence, the complexes may be regarded as non-electrolytes [21].

3.2. IR spectral studies

The IR spectrum of L showed a broad band at 3400 cm^{-1} due to phenolic OH and medium intensity weak bands at 3329 and 3200 cm^{-1} due to amide NH and NH attached to the thiazole moiety, respectively. The high intensity strong bands observed at 1699, 1624 and 1297 cm^{-1} are due to carbonyl function ν(C=O), azomethine function ν(C=N) and phenolic C-O, respectively.

In the IR spectra of all the metal complexes, it was observed that, the absence of absorption band due to phenolic OH at 3400 cm^{-1} of ligand indicates the formation of a coordination bond between the metal ion and phenolic oxygen atom *via* deprotonation. This is further confirmed by the increase in absorption frequency about 4-56 cm^{-1} of phenolic ν(C-O) which appeared in the region 1301-1353 cm^{-1} in all the metal complexes indicating the participation of oxygen atom of phenolic OH in the coordination. In the IR spectra of the metal complexes, medium intensity weak bands at 3319-3341 and 3196-3253 cm^{-1} were due to amide NH and NH attached to thiazole moiety, respectively, which appeared almost at about the same position as in the case of ligand, thus confirming their non-involvement in coordination. The shift of amide carbonyl ν(C=O) to lower frequency side about 12-82 cm^{-1} which appeared in the region 1617-1687 cm^{-1} in all the complexes confirms the coordination of oxygen atom of amide ν(C=O) with the metal ions as such without undergoing enolization [22,23]. The absorption frequency due to azomethine ν(C=N) function also shifted to the low frequency side about 20-78 cm^{-1} and appeared in the region 1546-1604 cm^{-1} suggesting the involvement of nitrogen atom of azomethine function in complexation with metal ions [14,24].

The coordination of metal ions with the Schiff base ligand was further confirmed by the appearance of new weak intensity, non-ligand bands in the region 533-588 and 432-455 cm^{-1} in all the complexes and 353 cm^{-1} in the case of zinc(II)

complex are assigned to frequencies of ν(M-O), ν(M-N) and ν(M-Cl) stretching vibrations respectively.

3.3. ^{1}H NMR spectral studies

The ^{1}H NMR spectrum (Figure S1) of L displayed three singlets each at δ 11.5, 10.9 and 10.6 ppm are due the proton of phenolic OH, amide NH and NH attached to thiazole moiety, respectively. The signal due to azomethine proton (CH=N) resonated as singlet at δ 8.1 ppm. The signals due to nine aromatic protons (ArH) have resonated as multiplets in the region δ 6.1-7.8 ppm and signals at δ 3.2 and 1.3 ppm are due to four and six protons of two CH_2 and two CH_3 groups respectively. The L upon complexation with zinc(II) ion showed the disappearance of signal due to the proton of phenolic OH confirms the involvement of bonding of phenolic oxygen to metal ion *via* deprotonation. The signals due to amide NH and NH of thiazole are appeared in the region δ 11.9 and 11.1 ppm, respectively. The signal due to azomethine proton (CH=N) resonated at δ 8.4 ppm. The signals due to nine aromatic protons (Ar-H) have resonated as multiplets in the region δ 6.1-8.2 ppm and signals at δ 3.3 and 1.3 ppm are due to four and six protons of two CH_2 and two CH_3 groups, respectively. When compared to the ^{1}H NMR spectral data of L and its zinc(II) complex, all the signals due to protons have been shifted towards down field strength confirming the complexation of zinc(II) ion with the ligand.

3.4. ESI-mass spectral studies

3.4.1. Mass spectral fragmentation pattern study of L

The ESI mass spectrum of L exhibited M^+ +1 peak at *m/z* 410 (48%). The molecular ion peak M^+ 409, underwent fragmentation in two routes. In the first route, the fragmentation is observed due to loss of $C_9H_7N_2S$ radical of thiazole moiety and gave a fragment ion peak recorded at *m/z* 234 (14%). This fragment ion, on loss of CHN_2O radical gave a fragment ion peak recorded at *m/z* 177 (10%). In a another route, the molecular ion undergone fragment due to the loss of C_2H_2 molecule giving a fragment ion peak recorded at *m/z* 383 (100%) which is also a base peak. The schematic mass spectral fragmentation pattern is in consistency with its structure which is provided in Scheme 2.

3.4.2. Mass spectral fragmentation pattern study of copper(II) complex

The ESI mass spectrum of copper(II) complex showed M^+ +1 peak recorded at *m/z* 880 (3%). The molecular ion peak M^+ *m/z* 879 on loss of two $C_{10}H_6N_2OS$ molecule of thiazole moiety, CH_3 radical and a $H_2C{=}CH_2$ species gave a fragment ion peak recorded at *m/z* 432 (25%). This on further loss of a C_2H_5 radical, NH_2 radical and four hydrogen radicals gave a fragment ion peak recorded at *m/z* 383 (100%), which is also a base peak. The schematic mass spectral fragmentation pattern is in consistency with its structure which is illustrated in Scheme 3.

3.4.3. Mass spectral fragmentation pattern study of nickel(II) complex

The ESI mass spectrum of nickel(II) complex showed a molecular ion peak recorded at *m/z* 874 (7%) which is equivalent to its molecular weight. The molecular ion peak underwent fragmentation in two routes. In the first route, the molecular ion peak on the loss of a deprotonated ligand ($C_{21}H_{22}N_5O_2S$) molecule, a benzene molecule, five hydrogen radicals gave a fragment ion peak recorded at *m/z* 383 (100%), which is also a base peak. In another route, the molecular ion on the loss of a 4-phenylthiazole radical, a benzene molecule, three hydrogen radicals gave a fragment ion peak recorded at *m/z* 633 (3%). Further, this on loss of a diethylamine molecule of 4-(diethylamino) salicylaldehyde moiety and hydrogen radical gave a fragment ion peak recorded at *m/z* 559 (3%). The schematic mass spectral fragmentation pattern is in consistency with its proposed structure which is presented in Scheme 4.

3.4.4. Mass spectral fragmentation pattern study of zinc(II) complex

The ESI mass spectrum of zinc(II) complex showed a M^{+1} +1 peak recorded at *m/z* 508, 510 (3%, 1%), which is equivalent to its molecular weight. The molecular ion peak underwent fragmentation in two routes. In the first route, the sequential loss diethylamine molecule of 4-(diethylamino) salicylaldehyde moiety, 2-amino-4-phenylthiazole molecule and a coordinated chloride radical gave a fragment ion peak recorded at *m/z* 223 (19%). In another route, molecular ion peak on the loss of a hydrogen radical gave a fragment ion peak recorded at *m/z* 507, 509 (3%, 1%), this peak on further loss a hydrogen radical gave a fragment ion peak recorded at *m/z* 506, 508 (9%, 3%). This fragment ion on the loss of a C_6H_5 radical gave a fragment ion peak recorded at *m/z* 429, 431 (30%, 10%). Further, this on loss of two C_2H_5 radicals of 4-(diethylamino) salicylaldehyde moiety gave a fragment ion peak recorded at m/z 371, 373 (100%, 33%) which is also a base peak. This on simultaneous loss of and C_2HN species of thiazole moiety and a coordinated chloride radical gave a fragment ion peak recorded at *m/z* 297 (15%). The schematic mass spectral fragmentation pattern of zinc(II) complex is in consistency with its proposed structure which is provided in Scheme 5.

3.5. Electronic spectral studies

The electronic spectra of green colored copper(II) complex displayed a low intensity single broad asymmetric band in the region 15696-18146 cm^{-1}. The broadness of the band designates the three transitions $^2B_{1g} \rightarrow {}^2A_{1g}$ (ν_1), $^2B_{1g} \rightarrow {}^2B_{2g}$ (ν_2) and $^2B_{1g} \rightarrow {}^2E_g$ (ν_3), which are similar in energy and give rise to only one broad band and the broadness of the band may be due to dynamic Jahn-Teller distortion. The obtained data suggest the distorted octahedral geometry around the copper(II) ion [25].

The brown colored cobalt(II) complex under present study displayed two absorption bands at 16692 and 20493 cm^{-1}. These bands are assigned to be $^4T_{1g}$ (F) → $^4A_{2g}$ (F) (ν_2) and $^4T_{1g}$ (F) → $^4T_{2g}$ (P) (ν_3) transitions, respectively, which are in good agreement with the literature values for octahedral geometry [26]. The lowest band, ν_1 could not be observed due to the limited range of the instrument used, but it could be calculated using the band fitting procedure suggested by Underhill and Billing [27]. The calculated ν_1 value is presented in Table 1. The transition values of ν_1, ν_2 and ν_3 suggest the octahedral geometry for the cobalt (II) complex.

The brown colored nickel (II) complex under present investigation exhibited two absorption bands in the region 14897 and 25117 cm^{-1}, which are assigned to $^3A_{2g} \rightarrow {}^3T_{1g}$ (F) (ν_2) and $^3A_{2g}$ (F) → $^3T_{1g}$ (P) (ν_3) transitions respectively in an octahedral environment [28]. The transition value of band ν_1 was calculated by using a band fitting procedure [27].

The proposed octahedral geometry for copper(II), cobalt(II) and nickel(II) complexes was further supported by the calculated values of ligand field parameters, such as Racah inter electronic repulsion parameter (B'), nephelauxetic parameter (β), ligand field splitting energy (10 Dq) and ligand field stabilization energy (LFSE) [29]. The calculated B' values for the copper(II) and nickel(II) complexes are lower than the free ion values, which is due to the orbital overlap and delocalization of d-orbitals.

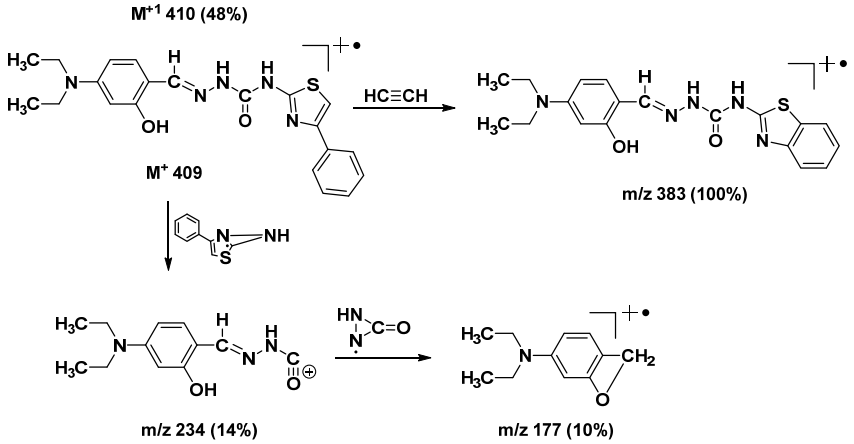

Scheme 2

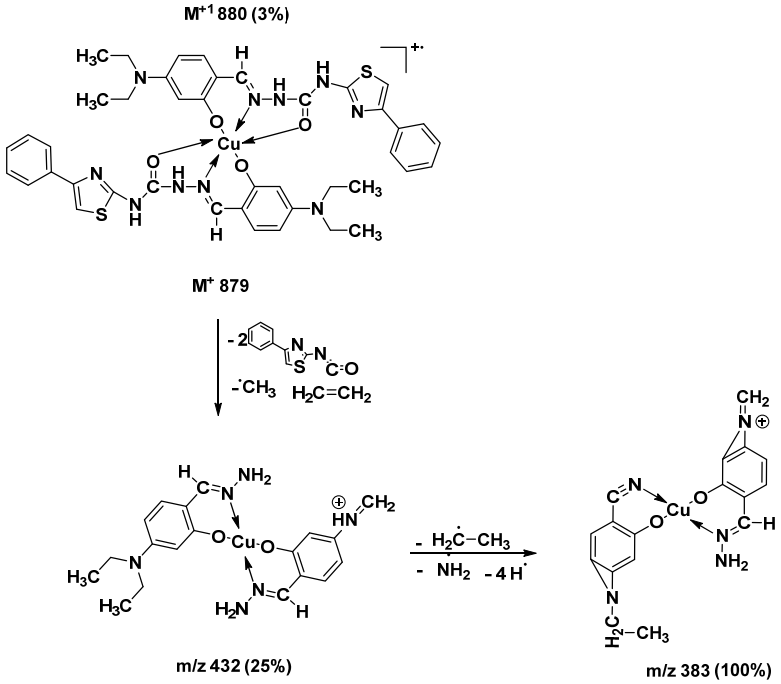

Scheme 3

The β values are important in determining the covalency for the metal-ligand bond and they were found to be less than unity, suggesting a considerable amount of covalency for the metal-ligand bonds. The β value for the nickel(II) complexes was less than that of the cobalt (II) complexes, indicating the greater covalency of the metal-ligand (M-L) bond.

3.6. Magnetic susceptibility studies

The obtained magnetic moment value for copper(II) complex is 1.85 BM. The obtained value is slightly higher than the spin-only value 1.73 BM due to one unpaired electron, suggesting the octahedral geometry for copper(II) complex [30]. Thus, the present complex is devoid of any spin interaction with distorted octahedral geometry. In octahedral cobalt(II) complex the ground state is $^4T_{1g}$. A large orbital contribution to the singlet state lowers the magnetic moment values for the various cobalt(II) complexes which are in the range 4.12-4.70 BM for tetrahedral and 4.70-5.20 BM for octahedral geometry of the complexes, respectively [31]. In the present study the observed magnetic moment value 5.06 BM suggests the octahedral geometry. Further, the observed magnetic moment value for nickel (II) complex is 2.93 BM, which is also well within the expected range of 2.83-3.50 BM, suggesting the consistency with its octahedral environment [32].

3.7. ESR spectral study of copper(II) complex

The ESR spectrum provides the evidence about the environment of the metal ion within the complex, i.e., the geometry and nature of the ligating sites of the ligand and metal ion.

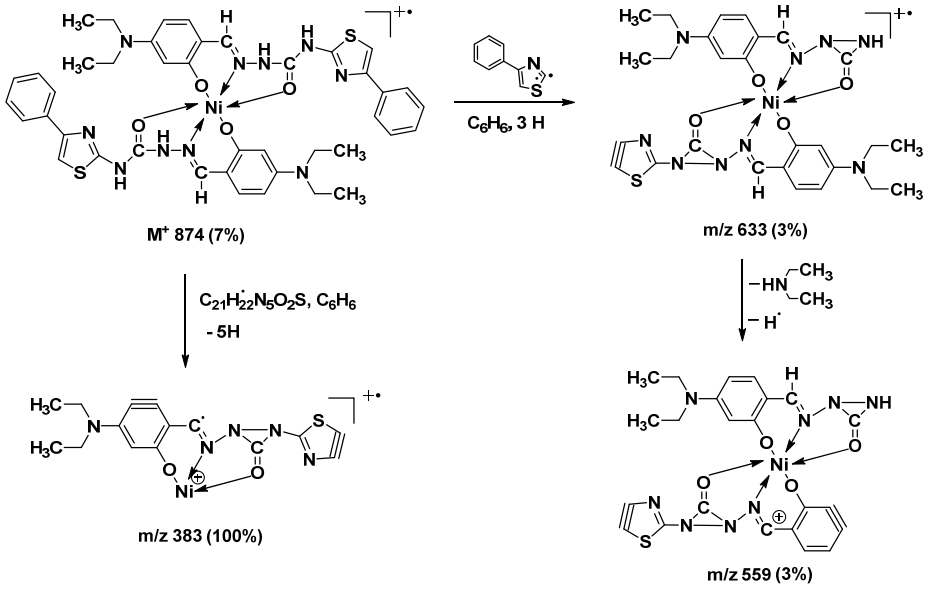

Scheme 4

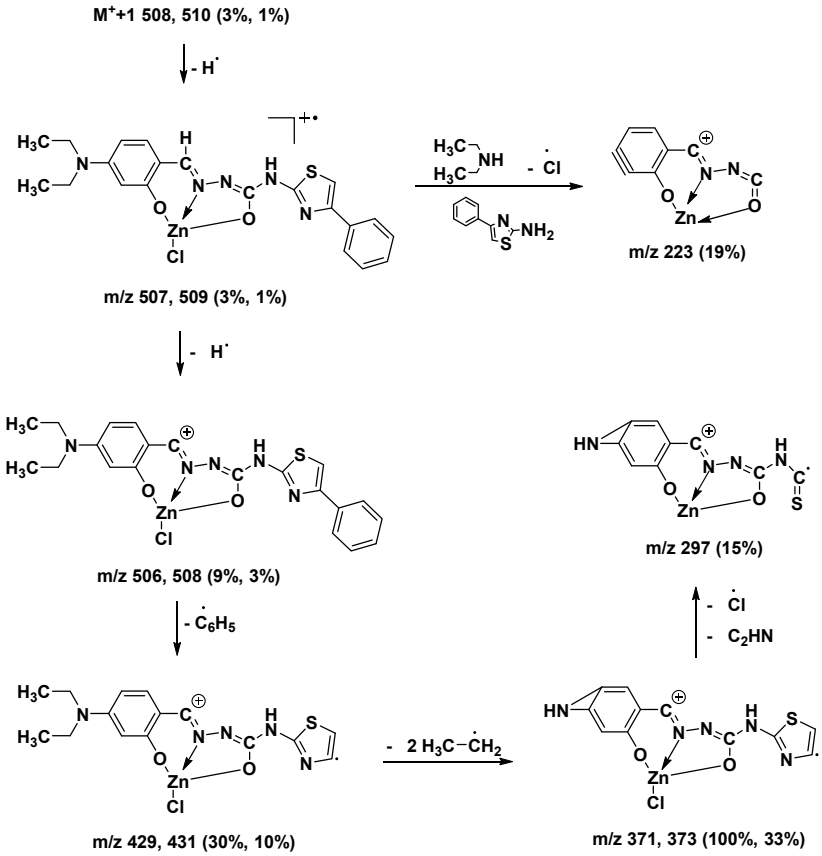

Scheme 5

In octahedral geometry with the g-tensor parameter $g_{\perp} > g_{||} > 2.0023$, the unpaired electron lies in the d_{z^2} orbital and $g_{||} > g_{\perp} > 2.0023$, the unpaired electron lies in the $d_{x^2-y^2}$ orbital in the ground state [33]. The observed measurements of copper(II) complex is $g_{||}$ (2.1467) > $g_{\perp}$ (2.0349) > 2.0023 indicate that the complex is axially symmetric and copper site has a $d_{x^2-y^2}$ ground state characteristic of octahedral geometry [34]. The $g_{||}$ value is an important function for indicating the metal-ligand (M-L) bond character, for covalent and ionic character $g_{||}$ value < 2.3 and $g_{||}$ value > 2.3, respectively [33].

Table 1. Electronic spectral data and ligand field parameters of copper(II), cobalt(II) and nickel(II) complexes.

Metal Complexes	Transitions in cm^{-1}			Dq (cm^{-1})	B′ (cm^{-1})	β	β%	ν_2/ν_1	LFSE (k.cal)
	ν_1^*	ν_2	ν_3						
Copper(II)		15696 - 18146		--	--	--	--	--	29.00
Cobalt(II)	7782	16692	20493	891	924	0.951	4.84	2.14	15.27
Nickel(II)	9130	14897	25117	913	841	0.808	19.13	1.63	31.30

Table 2. Thermal degradation pattern of metal(II) complexes.

Metal Complexes	Decomposition temp. (°C)	Weight loss (%)		Metal oxide (%)		Inference
		Obs.	Calc.	Obs.	Calc.	
Copper(II)	318	7.39	8.18	-	-	Loss due to $C_4H_{10}N$ species of 4-(diethylamino)salicylaldehyde
	370	43.89	43.86	-	-	Loss due to two moles of 2-amino-4-phenylthiazlole
	450	5.71	6.61	-	-	Loss due to two CH_3 groups.
	Up to 734	-	-	10.19	11.48	Loss due to remaining organic moiety
Cobalt(II)	209	16.29	16.45	-	-	Loss due to two moles of $C_4H_{10}N$ species of 4-(diethylamino)-salicylaldehyde
	282	18.58	21.06	-	-	Loss due to two phenyl groups of thiazole moieties
	418	63.04	62.05	-	-	Loss due to $C_{11}H_7N_4O_2S$ and $C_3H_3N_2S$ molecules.
	Up to 731	-	-	11.14	12.29	Loss due to remaining organic moieties.
Nickel(II)	160	8.14	8.23	-	-	Loss due to $C_4H_{10}N$ species of 4-(diethylamino)-salicylaldehyde
	300	20.16	19.43	-	-	Loss due to two benzene groups of thiazole moieties
	400	58.58	57.79	-	-	Loss due to $C_{11}H_{14}NO$ and $C_3H_2N_2S$ groups of 4-(diethyl-amino)salicylaldehyde and thiazole moiety respectively.
	492	36.58	35.67	-	-	Loss due to NCO and NHNCO groups.
	Up to 731	-	-	10.12	11.20	Loss due to remaining organic moiety.
Zinc(II)	254	8.51	6.88	-	-	Loss due to a coordinated chlorine atom.
	309	49.97	52.38	-	-	Loss due to a 2-amino-4-phenylthiazlole and $C_4H_{10}N$ group of 4-(diethylamino) salicylaldehyde
	388	52.48	52.34	-	-	Loss due to C_7H_4NO species.
	Up to 632	-	-	11.27	12.20	Loss due to remaining organic moiety.

Table 3. Powder X-ray data of copper(II) complex.

Peak	2θ	θ	Sinθ	$Sin^2\theta$	1000 $Sin^2\theta$	1000 $Sin^2\theta/CF$ ($h^2+k^2+l^2$)	h k l	d		a in Å
								Obs.	Calc.	
1	27.027	13.513	0.233	0.0546	54.603	1.00 (1)	1 0 0	3.299	3.304	3.295
2	34.965	17.482	0.300	0.0902	90.248	1.65 (2)	1 1 0	2.566	2.566	3.293
3	50.782	25.391	0.428	0.1838	183.863	3.36 (3)	1 1 1	1.797	1.799	3.292
4	56.857	28.428	0.476	0.2266	226.634	4.15 (4)	2 0 0	1.619	1.617	3.295
5	60.449	30.224	0.503	0.2534	253.400	4.64 (5)	2 1 0	1.531	1.530	3.294

In the present case, $g_{||}$ value is < 2.3, indicating an appreciable covalent character of the metal-ligand (M-L) bond. The geometric parameter (G) is the measure of extent of exchange interactions and is calculated by using the g-tensor values by using the expression $G = g_{||} - 2.0023/g_{\perp} - 2.0023$. According to Hathaway and Billing [35], if the G value is greater than 4, the exchange interaction between the copper centers is negligible, whereas if its value is less than 4 and the exchange interaction is noticed. In the present investigations, it was found that the G value of the copper(II) complex is 4.43, indicate the exchange coupling effects are not operative.

3.8. Thermal studies

The thermogram of copper(II) complex showed that the complex is stable up to 317 °C and no weight loss occurs before this temperature. The complex underwent degradation in three successive stages. The first stage of degradation occurred at 318 °C, due to the loss of $C_4H_{10}N$ species of 4-(diethylamino) salicylaldehyde with a practical weight loss of 7.39% (Calcd. 8.18%). The resultant complex on further degradation gave a break at 370 °C by the loss of two moles of 2-amino-4-phenylthiazlole with a practical weight loss of 43.89% (Calcd. 43.86%). Further, the resultant complex underwent third stage of decomposition at 450 °C due to the loss of two CH_3 groups with a practical weight loss of 5.71% (Calcd. 6.61%). Further, complex showed gradual decomposition up to 734 °C and onwards due to the loss of remaining organic moiety. The final weight of the residue corresponds to cupric oxide.

Similarly, cobalt(II), nickel(II) and zinc(II) complexes underwent a decomposition in three, four and three successive stages, respectively, and the final weight of the residue corresponds to the formation of respective metal oxides. The proposed stepwise degradation pattern of all the complexes at different stages are due to the loss of different organic moieties, with respect to temperature, which is illustrated in Table 2.

3.9. Powder X-ray diffraction studies (Powder-XRD)

Though our newly synthesized metal complexes were soluble in some polar organic solvents like DMSO and DMF, crystals that are appropriate for single crystal studies are not achieved. In order to test the degree of crystallinity of metal complexes, we obtained the powder X-ray diffraction pattern for all the metal (II) complexes. In the powder X-ray diffraction pattern of all the complexes, it was observed that the trend of curves decreases from maximum to minimum intensity indicating the amorphous nature of the complexes.

Powder X-ray diffraction pattern of copper(II), cobalt(II), nickel(II) and zinc(II) complexes displayed a five, five, four and six reflections respectively, with maxima at 2θ = 60.449, 60.546, 60.431 and 64.433 ° corresponding to observed d values 3.294, 3.290, 2.947 and 2.567 Å, respectively. Bragg's equation ($n.\lambda = 2.d.\sin\theta$) was used for calculating the inter-planar spacing (d). The calculated inter-planar *d*-spacing together with relative intensities with respect to most intense peak have been recorded. From all the highly intense peaks, unit cell calculations have been calculated for all the complexes and $h^2 + k^2 + l^2$ values were also determined. The observed inter-planar d-spacing values have been compared with the calculated ones and it was found to be in good agreement with experimental values. The $h^2+k^2+l^2$ values of copper (II) complex are 1, 2, 3, 4 and 5, also the calculated lattice parameter is a = b = c = 2.950 Å. From the Table 3, it was observed that the absence of forbidden numbers (7, 15, 23, etc.) indicates that the complex belongs to cubic symmetry.

Table 4. Antibacterial and antifungal activity results, zone of inhibition in mm.

Bacteria/Fungi	Ligand/Complexes	Concentration (µg/mL)						
		25	50	100	250	500	1000	MIC
S. aureus	L	0	0	0	7	10	13	250
	Copper(II)	0	0	8	10	16	20	100
	Cobalt(II)	0	0	0	6	12	15	250
	Nickel(II)	0	0	0	5	9	14	250
	Zinc(II)	0	0	4	6	9	13	100
E. coli	L	0	0	0	6	12	17	250
	Copper(II)	0	0	7	11	17	21	100
	Cobalt(II)	0	0	0	5	11	15	250
	Nickel(II)	0	0	6	10	16	21	100
	Zinc(II)	0	0	4	8	11	17	100
A. Flavus	L	0	0	0	0	8	17	500
	Copper(II)	0	0	9	15	21	29	100
	Cobalt(II)	0	0	0	7	13	17	250
	Nickel(II)	0	0	0	0	8	15	500
	Zinc(II)	0	0	8	13	19	25	100
A. niger	L	0	0	9	13	19	26	100
	Copper(II)	0	0	7	13	17	24	100
	Cobalt(II)	0	0	0	0	10	17	500
	Nickel(II)	0	0	0	0	9	17	500
	Zinc(II)	0	0	9	16	24	29	100
Ciproflaxacin *		**	**	**	**	**	**	**
Fluconazole *		**	**	**	**	**	**	**

* Broad spectrum antibiotics for bacterial/fungal strains.
** The inhibitions zones were too big to measure.

Similar calculations were done for cobalt(II), nickel(II) and zinc(II) complexes and all the important peaks have been indexed and observed values of inter-planar distances (d) have been compared with the calculated ones and it was found to be in good agreement. It was observed that the absence of forbidden numbers (7, 15, 23, etc.) in indicates that complexes belong to cubic symmetry.

3.10. Biological evaluations

3.10.1. Antibacterial and antifungal assay results

The newly synthesized L and its metal(II) complexes have been evaluated for their antibacterial and antifungal activity. The MIC values of the tested compounds against the respective bacterial and fungal strains along with the standards are summarized in Table 4.

In most of the cases, the metal complexes revealed good antimicrobial activity results than the free ligand. This activity found to be improved on coordination of the hetero atoms of the L with various metal ions. This enhancement in the antimicrobial activity of the complexes over the free ligand can be explained on the basis of chelation theory [36,37]. It is known that chelation enhances the ligand to act as more powerful and potent bactericidal/fungicidal agents by inhibiting the growth of bacteria/fungi, thus a zone of inhibition of metal complexes was found to be higher compared to the ligand [23]. The enhancement in the anti-microbial activity may be rationalized on the basis that ligands mainly possess azomethine (C=N) bond. Moreover, in metal complex, the positive charge of the metal ion is partially shared with the hetero donor atoms (N and O) present in the ligand and there may be π-electron delocalization over the whole chelating system [38]. Hence the increase in the lipophilic character of the metal chelates favour their permeation through the lipoid layer of the bacterial cell membranes and blocking of the metal binding sites in the enzymes of microorganisms. In general, metal complexes are more active than the ligands because metal complexes may serve as a vehicle for activation of ligands as the principal cytotoxic species [39].

3.10.2. In vitro cytotoxicity

The brine shrimp bioassay is an excellent tool to be used for monitoring the biological activity in order to predict the capability to kill cancer cells [40]. A summary of the cytotoxic assay results of the L and its metal(II) complexes is presented in Table 5. Among all the tested compounds zinc(II) and nickel(II) complexes showed the highest cytotoxicity with LD_{50} value of 1.148×10^{-4} and 1.216×10^{-4}, respectively. The L and its copper(II) and cobalt(II) complexes were found to be less active against *A. salina*.

Table 5. Brine shrimp bioassay data.

Compounds	LD_{50} (M/mL)
L	2.279×10^{-4}
Copper(II)	2.139×10^{-4}
Cobalt(II)	2.106×10^{-4}
Nickel(II)	1.216×10^{-4}
Zinc(II)	1.148×10^{-4}
Bleomycin	0.410×10^{-4}

3.10.3. Antioxidant assay (DPPH free radical scavenging activity)

To evaluate the antioxidant property, we studied their free radical scavenging ability using DPPH radical which reacts with an electron or hydrogen donor to become a stable diamagnetic molecule *viz.* hydrazine. The solution therefore loses color depending on the number of electrons accepted. A substance capable of donating electrons or hydrogen atom is able to convert the purple color of DPPH to its non-radical yellow color, form: 2,2-diphenyl-1-picrylhydrazyl, a reaction which can be followed spectrophotometrically [41,42]. The results in different concentrations are presented in Figure 1. Amongst the tested compounds, L and its cobalt(II) and zinc(II) complexes have showed good scavenging activity.

4. Conclusion

A series of copper(II), cobalt(II), nickel(II) and zinc(II) complexes were prepared with tridentate ONO donor Schiff base ligand (L) derived from *N*-(4-phenylthiazol-2-yl)-hydrazinecarboxamide and 4-(diethylamino)salicylaldehyde and characterized them by various spectral techniques. Spectral analysis indicates octahedral geometry for copper(II), cobalt (II) and nickel(II) complexes have a 1:2 stoichiometric ratio of the type $[M(L)_2]$ and zinc(II) complex has a 1:1 stoichiometry ratio of the type [ZnLCl]. Also the mass fragmentation patterns of the complexes are in consistency with proposed structures.

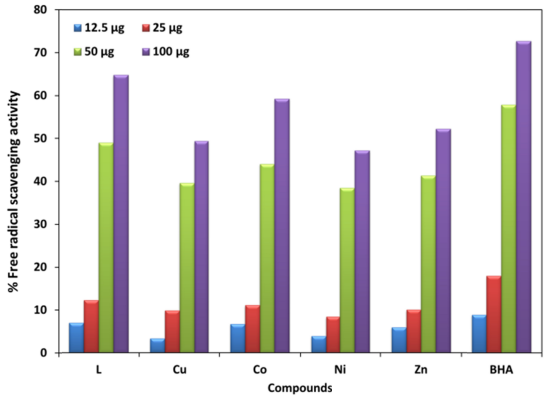

Figure 1. Antioxidant activity results.

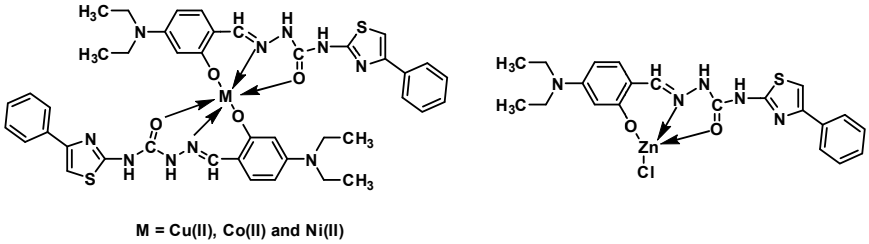

Figure 2. Proposed structures of the metal complexes.

The antimicrobial activity results showed that all the newly synthesized metal(II) complexes have exhibited higher activity when compared to the free ligand. This activity was increased upon chelation or coordination of the ligand with metal atoms. The chelation process reduces the polarity of metal ion by coordinating with ligand, which increases the lipophilic nature of the metals. This lipophilic nature of the metal enhanced its penetration through the lipoid layer of the cell membrane of the microorganism. In the present study the free ligand L showed good antioxidant activity when compared to the metal complexes and increased in the activity of the ligand is due to the presence of hydroxyl groups in the ligand. Hence, from all these extensive observations, it was concluded that the Schiff base ligand (L) and its metal complexes gave the remarkable, versatile and valuable information of coordination compounds about the study of bonding modes and elucidating the various structures of the metal complexes and also they may be used as potent biological agents with reduced toxicity and higher efficiency. Based on physicochemical evidences, we proposed the following geometry/structure (Figure 2) of the metal complexes.

Acknowledgements

One of the authors (Nagesh Gunvanthrao Yernale) is grateful to Department of Science and Technology, New Delhi for the award of DST-INSPIRE SRF [DST/AORC-IF/UPGRD/ 2014-15/IF120091]. The authors extend their thanks to Indian Institute of Technology Bombay, Sophisticated Test and Instrumentation Centre, Cochin University, Sophisticated Analytical Instrumentation Facility, Panjab University, for providing spectral data. Authors are also thankful for BioGenics Research and Training Centre in Biotechnology, Hubli for biological studies.

References

[1]. Hossein, N.; Mohsen, M. *J. Chem.* **2013**, 701826, 1-8.
[2]. Ikechukwu, P. E.; Peter, A. A. *Molecules* **2015**, *20*, 9788-9802.
[3]. Reda, A. A. A.; Abdel-Nasser, M. A. A. *Int. J. Electrochem. Sci.* **2013**, *8*, 8686-8699.
[4]. Richard, H. H.; Pierre, K.; Edward, I. S. *Chem. Rev.* **1996**, *96*, 2239-2314.
[5]. Yuanyuan, C.; Erik, R. F. ; Mark, R. C. ; Krzysztof, P.; Philip, D. K. *J. Biol. Chem.* **2012**, *287*, 13356-13370.
[6]. Joseyphus, R. S.; Sivasankaran, N. M. *Arabian J. Chem.* **2010**, *3*, 195-204.
[7]. Yoshihisa, K.; Naoyuki, M.; Michihiro, K.; Takashi, H.; Daisuke, Y.; Hiroshi, S.; Yuya, H.; Makoto, H.; Masahiro, M. *Chem. Pap.* **2014**, *68*, 923-931.
[8]. Xu, Z.; Ba, M.; Zhou, H.; Cao, Y.; Tang, C.; Yang, Y.; He, R.; Liang, Y.; Zhang, X.; Li, Z.; Zhu, L.; Guo, Y.; Guo, C. *Eur. J. Med. Chem.* **2014**, *6*, 27-42.
[9]. Leyla, Y.; Yusuf, O.; Hulya, K. G.; Ulviye, A. *J. Chem.* **2015**, 464379, 1-7.
[10]. Yernale, N. G.; Mruthyunjayaswamy, B. H. M. *Bioinorg. Chem. Appl.* **2014**, 314963, 1-17.
[11]. Maya, S. S.; Sushobhan, C. *RSC Advances* **2012**, *2*, 4547-4592.
[12]. Kiran, S.; Yogender, K.; Parvesh, P.; Gulab, S. *Bioinorg. Chem. Appl.* **2012**, 729708, 1-9.
[13]. *Basavarajaiah,* S. M.; *Mruthyunjayaswamy, B. H. M. Indian. J. Chem.* **2010**, *49B*, 1117-1126.
[14]. Nagesh, G. Y.; Raj, K. M.; Mruthyunjayaswamy, B. H. M. *J. Mol. Struct.* **2015**, *1079*, 423-432.
[15]. Vogel, A. I, Quantitative Inorganic Analysis Including Elemental Instrumental Analysis, 2th edition, London, 1962.
[16]. Threlfall, E. J.; Fisher, I. S. T.; Ward, L.; Tschape, H.; Gerner-Smidt, P. *Microb. Drug resist.* **1999**, *5*, 195-199.
[17]. Prescott, J. F.; Baggot, J. D.; Walker, R. D.; eds. Ames, I. A, Antimicrobial susceptibility testing and interpretation of results. *In:* Antimicrobial Therapy in Veterinary Medicine, Iowa State University Press, 12-26.
[18]. Meyer, B. N.; Ferrigni, N. R.; Putnam, J. E.; Jacobsen, L. B.; Nichols, D. E.; *McLaughlin. Planta. Med.* **1982**, *45*, 31-34.
[19]. Finney, D. J. Probit Analysis, Cambridge University Press, United Kingdom, 1971.
[20]. Singh, R. P.; Murthy, K. C. N.; Jayaprakasha, G. K. *Agric. Food Chem.* **2002**, *50*, 81-82.
[21]. Geary, W. J. *Coord. Chem. Rev.* **1971**, *7*, 81-122.
[22]. Roy, S.; Mandal, T. N.; Das, K.; Butcher, R. J.; Rheingold, A. L.; Kar, S. K. *J. Coord. Chem.* **2010**, *3*, 2146-2157.
[23]. Nagesh, G. Y.; Mahadev, D. U.; Mruthyunjayaswamy, B. H. M. *Int. J. Pharm. Sci. Rev. Res.* **2015**, *31*, 190-197.
[24]. Chandra, S.; Gupta, L. K. *Spectrochim. Acta A* **2005**, *62*, 1102-1106.

[25]. Liu, H.; Wang, H.; Gao, F.; Niu, D.; Lu, Z. *J. Coord. Chem.* **2007**, *60*, 2671-2678.
[26]. Rai, R. A. *J. Inorg. Nucl. Chem.* **1980**, *43*, 450-453.
[27]. Underhill, A. E.; Billing, D. E. *Nature,* **1966**, *210*, 834-835.
[28]. Bayoumi, H. A.; Alaghaz, A. M. A.; Aljahdali, M. S. *Int. J. Electrochem. Sci.* **2013**, *8*, 9399-9413.
[29]. Satyanarayana, D. N. Electronic Absorption Spectroscopy and Related Technique, University Press India Limited, New Delhi, 2001.
[30]. Singh, D. P.; Kumar, R.; Malik, V.; Tyagi, P. *Trans. Met. Chem.* **2007**, *32*, 1051-1055.
[31]. Baranwal, B. P.; Gupta, T. *Synth. React. Inorg. Met-Org. Chem.* **2004**, *32*, 1737-1754.
[32]. Rao, T. R.; Archana, P. *Synth. React. Inorg. Met-Org. Chem.* **2005**, *35*, 299-304.
[33]. Thaker, B. T.; Tandel, P. K.; Patel, A. S.; Vyas, C. J.; Jesani, M. S.; Patel, D. M. *Indian J. Chem.* **2005**, *44A*, 265-270.
[34]. Abdallah, S. M.; Zayed, M. A.; Mohamad, G. G. *Arab. J. Chem.* **2010**, *3*, 103-113.
[35]. Hathaway, B. J.; Billing, D. E. *Coord. Chem. Rev.* **1970**, *5*, 143-207.
[36]. Chohan, Z. H.; Arif, M.; Akhtar, M. A.; Supuran, C. T. *Bioinorg. Chem. Appl.* **2006**, 83131, 1-13.
[37]. Nagesh, G. Y.; Mruthyunjayaswamy, B. H. M. *J. Mol. Struct.* **2015**, *1085*, 198-206.
[38]. Abd El-Wahab, Z. H.; Mashaly, M. M.; Salman, A. A.; El-Shetary, B. A.; Faheim, A. A.; *Spectrochim. Acta A* **2004**, *60*, 2861-2873.
[39]. Petering, D. H.; Sigel, H. Metal Ions in Biological Systems, Marcel Dekker, New York, 1980.
[40]. Hartl, M.; Humpf, H. U.; *Food Chem. Toxicol.* **2000**, *38*, 1097-1102.
[41]. Mahendra, R. K.; Vivekanand, B.; Nagesh, G. Y.; Mruthyunjayaswamy, B. H. M. *J. Mol. Struct.* **2014**, *1059*, 280-293.
[42]. Satyendra, M.; Shailendra, K. J.; Avadhesha, S. *Electrochim. Acta* **2015**, *151*, 574-583.